

A New Modification of Rani Distribution with More Flexibility in Application

Harrison O. Etaga¹, Chrisogonus K. Onyekwere¹, Dorathy O. Oramulu¹, Okechukwu J. Obulezi^{1*}

¹Department of Statistics, Faculty of Physical Sciences, Nnamdi Azikiwe University, Awka, Nigeria

DOI: [10.36347/sjpms.2023.v10i07.003](https://doi.org/10.36347/sjpms.2023.v10i07.003)

| Received: 22.08.2023 | Accepted: 26.09.2023 | Published: 30.09.2023

*Corresponding author: Okechukwu J. Obulezi

Department of Statistics, Faculty of Physical Sciences, Nnamdi Azikiwe University, Awka, Nigeria

Abstract

Review Article

In this article, the Rani distribution has been modified to a more flexible variant. The new model is called "the XRani distribution" and it is also a one-parameter distribution just as the parent distribution-Rani. The properties of the XRani distribution were derived and an analysis of the behaviour was conducted. The parameter was estimated using the maximum likelihood procedure. Four lifetime data sets were used to illustrate the importance of the proposed model. From the results, the proposed model competes favorably among the members of the Lindley class of distributions.

Keywords: Exponential distribution, goodness of fit, model performance, Rani distribution, XRani distribution

Copyright © 2023 The Author(s): This is an open-access article distributed under the terms of the Creative Commons Attribution 4.0 International License (CC BY-NC 4.0) which permits unrestricted use, distribution, and reproduction in any medium for non-commercial use provided the original author and source are credited.

1. INTRODUCTION

The need for the development of new distributions has been on the rise as more and more complex data are encountered. Development of distributions started early enough that as of today, the numbers of existing distributions are countless. The rising quest for complex statistical analysis in medical and biological sciences has supported the development of probability models that are tailored toward modeling real-life data. [12] introduced a model widely applied in many fields. The model integrated exponential distribution with parameter θ and gamma distributions $(2, \theta)$. To further emphasize the significance of Lindley distribution, [9] provided its mathematical characteristics and showed that they are more flexible than that of the exponential distribution. Many extensions of Lindley distribution exist in many literature. Check out the following articles [1, 3, 28], others, for more information. Essentially, [18], a mathematically tractable member of Lindley class of distributions with extensions [10, 15, 16, 19]. The aim of developing new distributions is to increase flexibility and robustness, so as to enable the modeling and description of lifetime data sets arising from new situations. Some of the models were developed either by adding new parameters to existing ones, for instance, [2, 6, 8, 14], or

by forming a baseline distribution. However, whichever method one wants to adopt in generating a new model, the interest should center on keeping the model simple while increasing flexibility. Keeping this in mind, the interest of the authors in this article is to introduce a more flexible version of Rani's distribution, known as "The XRani distribution", to study the characteristics and demonstrate its applications in modeling lifetime data sets. Rani distribution developed by [24], is a one-parameter distribution for modeling lifetime data sets. Rani distribution is a mixture of exponential (θ) and gamma ($5, \theta$), with mixing proportion $p = 0.5\theta + 5.24$. Some extensions of Rani distribution can be found in the following articles [4, 17, 29], others. Having stated the aim of this article, the rest of this article shall be structured as follows: In section 2, the suggested XRani distribution is specified with the behavior studied. In section 3, we derive some of the properties. In section 4, we apply the distribution to four-lifetime data sets and demonstrate that the proposed distribution is useful among the Lindley class of distributions. The article is concluded in section 5.

2. The proposed XRani distribution

Let $X \sim \text{XRani}(\theta)$, then the pdf and cdf are respectively given by

$$f(x) = \frac{\theta^5}{(\theta^5 + 24)^2} [\theta^6 + 48\theta + 24x^4] e^{-\theta x}; \quad x > 0, \quad \theta > 0 \tag{1}$$

and

$$F(x) = 1 - \left\{ 1 + \frac{1}{(\theta^5 + 24)^2} [24\theta^4 x^4 + 96\theta^3 x^3 + 288\theta^2 x^2 + 576\theta x] \right\} e^{-\theta x} \tag{2}$$

The new distribution is obtained from the two-component mixture of exponential and Rani distributions with the same mixing proportion that yielded the Rani distribution. The mixture is of the form $p\text{Exp}(\theta) + (1-p)\text{Rani}(\theta)$. The shape of the distribution in figure 1

illustrates the flexibility with varying shapes using some theoretical parameter values.

The survival and hazard rate functions are respectively

$$S(x) = \left\{ 1 + \frac{1}{(\theta^5 + 24)^2} [24\theta^4 x^4 + 96\theta^3 x^3 + 288\theta^2 x^2 + 576\theta x] \right\} e^{-\theta x} \tag{3}$$

and

$$hrf(x) = \frac{\theta^{11} + 48\theta^6 + 24\theta^5 x^4}{\theta^{10} + 48\theta^5 + 576 + 24\theta^4 x^4 + 96\theta^3 x^3 + 288\theta^2 x^2 + 576\theta x} \tag{4}$$

The limiting values of the XRani hazard function are

$$\lim_{x \rightarrow 0} hrf(x) = \frac{\theta^{11} + 48\theta^6}{\theta^{10} + 48\theta^5 + 576} \quad \text{and} \quad \lim_{x \rightarrow \infty} hrf(x) = \theta$$

The plots are displayed in the figures 1, 2, 3, and 4 below

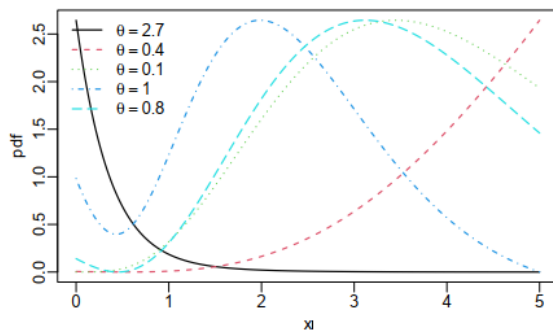


Figure 1: PDF of XRani distribution

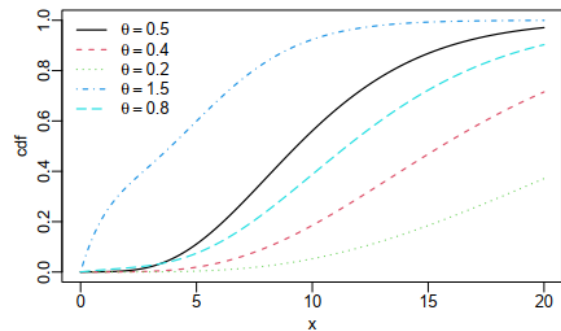


Figure 2: CDF of XRani distribution

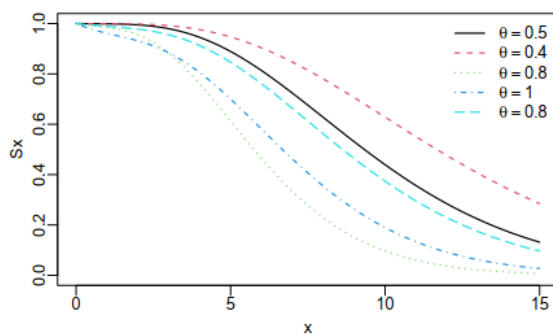


Figure 3: Survival Function of XRani distribution

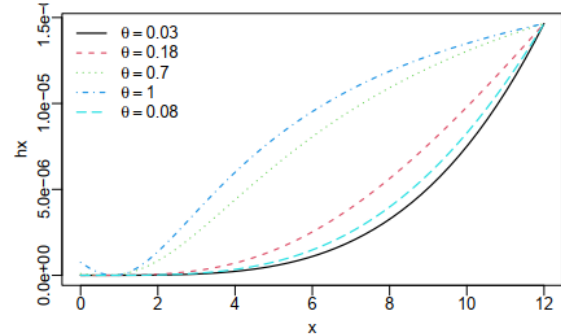


Figure 4: Hazard Function of XRani distribution

3 Mathematical Properties of the XRani distribution

In this section, we derive some essential properties of the proposed model.

3.1 Moments

Let $X \sim \text{XRani}(\theta)$ with pdf in eq 1, then the r th crude moment is given by

$$\mu'_r = \int_0^\infty x^r f(x) dx = \frac{\theta^{-r} \{24(r+4)! + \theta^{r+10} + 48\theta^{r+5}\}}{(\theta^5 + 24)^2}; \quad r = 1, 2, \dots \tag{5}$$

The mean of the XRani distribution is

$$\mu'_1 = \frac{2880 + 48\theta^5 + \theta^{10}}{\theta(24 + \theta^5)^2}; \tag{6}$$

The second, third, and fourth central moments are respectively

$$\mu'_2 = \frac{2(8640 + 48\theta^5 + \theta^{10})}{\theta^2(24 + \theta^5)^2}; \quad \mu'_3 = \frac{6(20160 + 48\theta^5 + \theta^{10})}{\theta^3(24 + \theta^5)^2}; \quad \text{and} \quad \mu'_4 = \frac{24(40320 + 48\theta^5 + \theta^{10})}{\theta^4(24 + \theta^5)^2} \tag{7}$$

For $X \sim \text{XRani}(\theta)$, the variance is

$$\sigma^2 = \mu'_2 - (\mu'_1)^2 = \frac{17280 - 2880\theta + 96\theta^5 - 48\theta^6 + 2\theta^{10} - \theta^{11}}{\theta^2(24 + \theta^5)^2} \tag{8}$$

The skewness (ζ), kurtosis (η), and coefficient of variation (ψ) are respectively

$$\zeta = \frac{6(\theta^{10} + 48\theta^5 + 20160)(24 + \theta^5)^4}{(1658880 + 608256\theta^5 + 14976\theta^{10} + 96\theta^{15} + \theta^{20})^{\frac{3}{2}}}; \quad \eta = \frac{24(24 + \theta^5)^6(40320 + 48\theta^5 + \theta^{10})}{(1658880 + \theta^5(48 + \theta^5)(12672 + 48\theta^5 + \theta^{10}))^2}, \tag{9}$$

and

$$\psi = \frac{\sqrt{1658880 + 608256\theta^5 + 14976\theta^{10} + 96\theta^{15} + \theta^{20}}}{(24 + \theta^5)^2(2880 + 48\theta^5 + \theta^{10})} \times \frac{100}{1}$$

The moment generating function and the characteristic function of the XRani distributed random variable X are given as

$$M_x(t) = E(e^{tx}) = \int_0^\infty e^{tx} f(x) dx = \frac{\theta^5(576 + (t - \theta)^2\theta(48 + \theta^5))}{(t - \theta)^5(24 + \theta^5)^2} \tag{10}$$

and

$$\phi_x(it) = E(e^{itx}) = \int_0^\infty e^{itx} f(x) dx = \frac{\theta^5(576 + (it - \theta)^2\theta(48 + \theta^5))}{(it - \theta)^5(24 + \theta^5)^2} \tag{11}$$

Table 1: Some theoretical statistics of the proposed distribution

θ	μ	μ'_2	μ'_3	μ'_4	σ^2	ζ	η	ψ
0.1000	50.0000	2999.9977	209999.8300	16799986.2000	500.0010	0.8944	-145.7990	0.4472
0.3071	16.2761	317.9421	7246.0603	188733.9791	53.0306	0.8932	-145.5281	0.4474
0.5143	9.6990	113.1093	1539.3666	23944.6771	19.0395	0.8787	-142.2816	0.4499
0.7214	6.8415	56.7759	550.5520	6103.7053	9.9699	0.8165	-128.1225	0.4615
0.9286	5.1471	33.0023	248.2358	2136.8671	6.5098	0.6838	-95.4449	0.4957
1.1357	3.9072	20.2056	123.7694	869.8061	4.9395	0.5669	-53.7435	0.5688
1.3429	2.8769	12.2240	62.7819	371.9223	3.9473	0.6251	-23.1074	0.6906
1.5500	2.0146	7.0168	30.6806	156.4000	2.9584	0.9089	-7.7931	0.8538
1.7571	1.3587	3.7933	14.1484	62.7711	1.9472	1.3628	-0.7327	1.0270
1.9643	0.9229	1.9928	6.2607	24.2136	1.1412	1.8992	3.6537	1.1576
2.1714	0.6636	1.0790	2.7830	9.2928	0.6385	2.3899	7.3834	1.2041
2.3786	0.5170	0.6378	1.3167	3.7218	0.3705	2.6776	10.0433	1.1773
2.5857	0.4325	0.4229	0.6959	1.6321	0.2359	2.6963	10.5656	1.1231
2.7929	0.3800	0.3114	0.4189	0.8114	0.1670	2.5441	9.2101	1.0754
3.0000	0.3441	0.2474	0.2833	0.4615	0.1290	2.3627	7.2849	1.0436

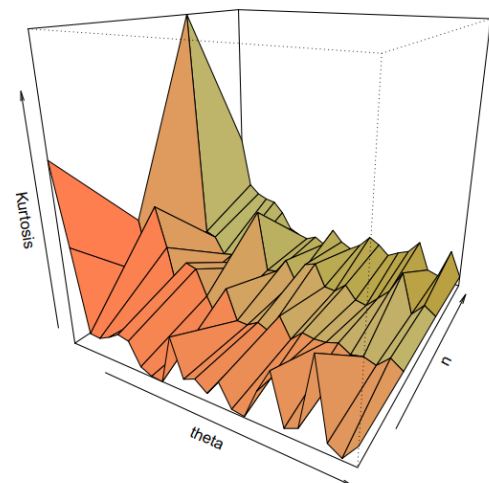
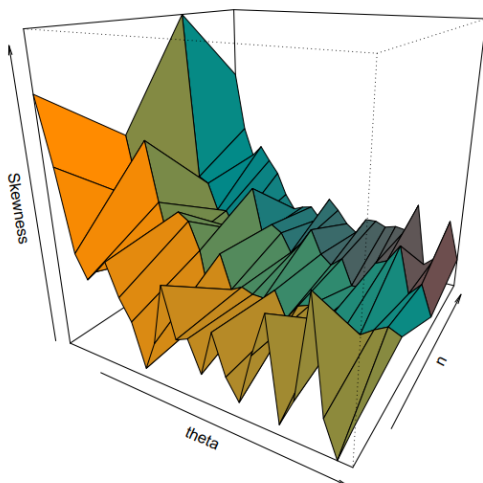


Figure 5: surface plot of the skewness for various n and θ **Figure 6:** surface plot of the kurtosis for various n and θ

3.2 Stochastic ordering of XRani distribution

The stochastic ordering of a nonnegative continuous random variable is a tool for comparing the behavior of system components. A random variable X is said to be smaller than another random variable Y in the stochastic order ($X \leq_{st} Y$) if $F_Y(x) \geq F_X(x) \forall x$. Hazard order ($X \leq_{hr} Y$) if $h_X(x) \geq h_Y(x) \forall x$. Mean residual life order ($X \leq_{mrl} Y$) if $m_X(x) \geq m_Y(x) \forall x$. Likelihood ratio order ($X \leq_{lr} Y$) if $\frac{f_X(x)}{f_Y(x)}$ decreases in x .

This implies that $X \leq_{lr} Y \Rightarrow X \leq_{hr} Y \Rightarrow X \leq_{st} Y \Rightarrow X \leq_{mrl} Y$

Theorem 1. Let $X \sim XRani(\theta_1)$ and $Y \sim XRani(\theta_2)$. if $\theta_1 \geq \theta_2$ then $X \leq_{lr} Y$ hence $X \leq_{lr} Y$ hence $X \leq_{hr} Y$, $X \leq_{mrl} Y$ and $X \leq_{st} Y$

$$\frac{f_x(x)}{f_y(x)} = \frac{\frac{\theta_1^5}{(\theta_1^5+24)^2}(\theta_1^6 + 48\theta_1 + 24x^4)e^{-\theta_1x}}{\frac{\theta_2^5}{(\theta_2^5+24)^2}(\theta_2^6 + 48\theta_2 + 24x^4)e^{-\theta_2x}} = \frac{\theta_1^5(\theta_2^5 + 24)^2(\theta_1^6 + 48\theta_1 + 24x^4)}{\theta_2^5(\theta_1^5 + 24)^2(\theta_2^6 + 48\theta_2 + 24x^4)} e^{(\theta_2 - \theta_1)x} \tag{12}$$

Taking a natural log of the ratio will yield

$$\ln \frac{f_x(x)}{f_y(x)} = \ln \frac{\theta_1^5(\theta_2^5 + 24)^2}{\theta_2^5(\theta_1^5 + 24)^2} + \ln \frac{\theta_1^6 + 48\theta_1 + 24x^4}{\theta_2^6 + 48\theta_2 + 24x^4} + (\theta_2 - \theta_1)x \tag{13}$$

Differentiating the natural log of the ratio w.r.t x will result

$$\frac{d}{dx} \ln \frac{f_x(x)}{f_y(x)} = \frac{96x^3(\theta_2^6 + 48\theta_2) - (\theta_1^6 + 48\theta_1)}{(\theta_2^6 + 48\theta_2 + 24x^4)(\theta_1^6 + 48\theta_1 + 24x^4)} + \theta_2 - \theta_1 \tag{14}$$

If $\theta_2 \geq \theta_1$, $\frac{d}{dx} \ln \frac{f_x(x)}{f_y(x)} \leq 0$, and $\frac{f_x(x, \theta_1)}{f_y(x, \theta_2)}$ is decreasing in x.

3.3 Bonferroni and Lorenz curve

The Bonferroni and Lorenz curves are defined as

$$B(p) = \frac{1}{p\mu} \int_0^q xf(x)dx = \frac{1}{p\mu} \left[\int_0^\infty xf(x)dx - \int_q^\infty xf(x)dx \right] = \frac{1}{p\mu} \left[\mu - \int_q^\infty xf(x)dx \right] \tag{15}$$

$$B(p) = \frac{\theta^6}{p(2880 + 48\theta^5 + \theta^{10})} \left[\frac{\theta^6 \gamma(2,q)}{\theta^2} + \frac{48\theta \gamma(2,q)}{\theta^2} + \frac{24 \gamma(6,q)}{\theta^6} \right]$$

and

$$L(p) = \frac{1}{\mu} \int_0^q xf(x)dx = \frac{1}{\mu} \left[\int_0^\infty xf(x)dx - \int_q^\infty xf(x)dx \right] = \frac{1}{\mu} \left[\mu - \int_q^\infty xf(x)dx \right] \tag{16}$$

$$L(p) = \frac{\theta^6}{(2880 + 48\theta^5 + \theta^{10})} \left[\frac{\theta^6 \gamma(2,q)}{\theta^2} + \frac{48\theta \gamma(2,q)}{\theta^2} + \frac{24 \gamma(6,q)}{\theta^6} \right]$$

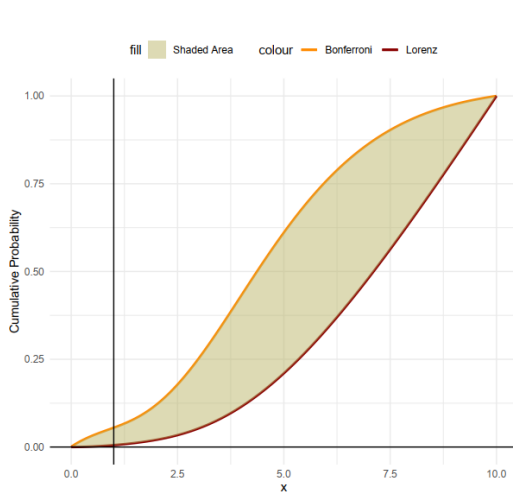


Figure 7: Bonferroni and Lorenz curves

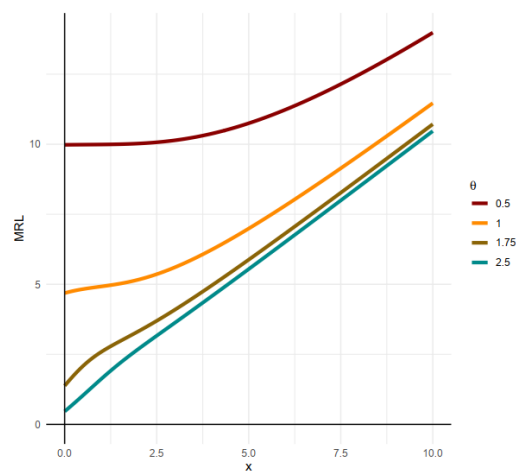


Figure 8: Mean Residual Life function plots for some θ

3.4 Mean Residual Life Function

The mean residual life function is defined as

$$f_{r;n}(x, \theta) = \frac{n!}{(r-1)!(n-r)!} f(x) [F(x)]^{r-1} [1-F(x)]^{n-r} = \frac{n!}{(r-1)!(n-r)!} \frac{\theta^5}{(\theta^5 + 24)^2} [\theta^6 + 48\theta + 24x^4] e^{-\theta x} \times \left[1 - \left\{ 1 + \frac{1}{(\theta^5 + 24)^2} [24\theta^4 x^4 + 96\theta^3 x^3 + 288\theta^2 x^2 + 576\theta x] \right\} e^{-\theta x} \right]^{r-1} \left[1 + \frac{1}{(\theta^5 + 24)^2} [24\theta^4 x^4 + 96\theta^3 x^3 + 288\theta^2 x^2 + 576\theta x] e^{-\theta x} \right]^{n-r} \tag{18}$$

The p.d.f of the largest order statistics is obtained by setting $r = n$

$$f_{n;n}(x, \theta) = \frac{n\theta^5}{(\theta^5 + 24)^2} [\theta^6 + 48\theta + 24x^4] e^{-\theta x} \left[1 - \left\{ 1 + \frac{1}{(\theta^5 + 24)^2} [24\theta^4 x^4 + 96\theta^3 x^3 + 288\theta^2 x^2 + 576\theta x] \right\} e^{-\theta x} \right]^{n-1} \tag{19}$$

The p.d.f of the smallest order statistic is obtained by

$$f_{1;n}(x, \theta) = \frac{n\theta^5}{(\theta^5 + 24)^2} [\theta^6 + 48\theta + 24x^4] e^{-\theta x} \left[1 + \frac{1}{(\theta^5 + 24)^2} [24\theta^4 x^4 + 96\theta^3 x^3 + 288\theta^2 x^2 + 576\theta x] e^{-\theta x} \right]^{n-r} \tag{20}$$

3.6 Renyi Entropy Measures

The entropy of a random variable is a measure of the variation of uncertainty. A popular entropy is the Renyi entropy. If X is a continuous random variable

having a probability density function, the Renyi entropy for $\omega \neq 1$ is given as:

$$\begin{aligned} R_\omega(x) &= \frac{1}{1-\omega} \log \int f(x)^\omega dx = \frac{1}{1-\omega} \log \int_0^\infty \left[\frac{\theta^5}{(\theta^5 + 24)^2} (\theta^6 + 48\theta + 24x^4) e^{-\theta x} \right]^\omega dx \\ &= \frac{1}{1-\omega} \log \frac{\theta^{5\omega}}{(\theta^5 + 24)^{2\omega}} \int_0^\infty (\theta^6 + 48\theta + 24x^4)^\omega e^{-\theta\omega x} dx \\ &= \frac{1}{1-\omega} \log \frac{\theta^{5\omega}}{(\theta^5 + 24)^{2\omega}} \int_0^\infty \sum_{j=0}^{\omega} \binom{\omega}{j} (\theta^6 + 48\theta)^j (24x^4)^{\omega-j} e^{-\theta x} dx \\ &= \frac{1}{1-\omega} \log \frac{\theta^{5\omega}}{(\theta^5 + 24)^{2\omega}} \sum_{j=0}^{\omega} \binom{\omega}{j} (\theta^6 + 48\theta)^j (24)^{\omega-j} \int_0^\infty x^{4\omega-4j} e^{-\theta x} dx \\ &= \frac{1}{1-\omega} \log \frac{1}{(\theta^5 + 24)^{2\omega}} \sum_{j=0}^{\omega} \binom{\omega}{j} (\theta^6 + 48\theta)^j (24)^{\omega-j} \theta^{\omega+4j-1} \frac{(4\omega-4j)!}{\omega^{4\omega-4j+1}} \end{aligned} \tag{21}$$

3.7 Odd Function

An odd function is a reliability tool for modeling data sets that show non-monotone. It is the ratio of the CDF to the survival function.

$$\begin{aligned} O(x; \theta) &= \frac{F(x; \theta)}{S(x; \theta)} = \frac{1 - \left\{ 1 + \frac{1}{(\theta^5 + 24)^2} [24\theta^4 x^4 + 96\theta^3 x^3 + 288\theta^2 x^2 + 576\theta x] \right\} e^{-\theta x}}{\left\{ 1 + \frac{1}{(\theta^5 + 24)^2} [24\theta^4 x^4 + 96\theta^3 x^3 + 288\theta^2 x^2 + 576\theta x] \right\} e^{-\theta x}} \\ &= \frac{24\theta^4 x^4 + 96\theta^3 x^3 + 288\theta^2 x^2 + 576\theta x}{(\theta^5 + 24)^2 + 24\theta^4 x^4 + 96\theta^3 x^3 + 288\theta^2 x^2 + 576\theta x} \end{aligned} \tag{22}$$

3.8 Stress-strength Reliability Analysis

The reliability of a system is the probability that its strength exceeds its stress. This reliability is called

stressstrength reliability. The inferences of the stress-strength reliability $R = P(X > Y)$ where Y is the stress and X is the strength.

$$\begin{aligned}
 R &= P(Y < X) = \int_0^\infty P(Y < X | X = x) f_x(x) dx = \int_0^\infty f(x; \theta_1) F(x; \theta_2) dx \\
 &= \frac{\theta_1^5}{(\theta_1^5 + 24)(\theta_2^5 + 24)} [\theta_1^5 \theta_2^{210} + 48\theta_2^5(\theta_1^5 + \theta_2^5) + 576(\theta_1^5 + \theta_2^5)] \\
 &\quad - \frac{\theta_1^6 \theta_2^{10} + 48\theta_1(\theta_1^5 \theta_2^5 + \theta_2^{10}) + 12\theta_1^5 + 48\theta_2^5 + 576}{(\theta_1 + \theta_2)^2} \frac{576\theta_1 \theta_2 (\theta_1^5 + 48)}{(\theta_1 + \theta_2)^3} \\
 &\quad - \frac{576\theta_1 \theta_2^2 (\theta_1^5 + 48)}{(\theta_1 + \theta_2)^4} - \frac{576\theta_2^4 (\theta_1^6 + \theta_2^6) + 27648\theta_2^4 (\theta_1 + \theta_2) + 331776}{(\theta_1 + \theta_2)^5} - \frac{576\theta_2^5 (\theta_2^5 + 48) + 331776}{\theta_1^5} \\
 &\quad - \frac{13824\theta_2 (5!)}{(\theta_1 + \theta_2)^6} - \frac{6912\theta_2^2 (6!)}{(\theta_1 + \theta_2)^7} - \frac{2304\theta_2^3 (7!)}{(\theta_1 + \theta_2)^8} - \frac{576\theta_2^4 (8!)}{(\theta_1 + \theta_2)^9}
 \end{aligned} \tag{23}$$

3.9 Maximum Likelihood Function

Let (x_1, x_2, \dots, x_n) be n random samples drawn from XRani distribution, the likelihood function is given as

$$\ell(f(x, \theta)) = \prod_{i=1}^n \frac{\theta^5}{(\theta^6 + 24)^2} \{\theta^6 + 48\theta + 24x^4\} e^{-\theta x} = \frac{\theta^{5n}}{(\theta^6 + 24)^{2n}} e^{-\theta \sum x} \prod_{i=1}^n \{\theta^6 + 48\theta + 24x^4\} \tag{24}$$

Taking the log of ℓ and differentiating with respect to θ yields the following results

$$\psi = 5n \ln \theta - 2n \ln(\theta^5 + 24) - \theta \sum x + \sum_{i=1}^n \ln(\theta^6 + 48\theta + 24x^4); \quad \frac{d\psi}{d\theta} = \frac{5n}{\theta} - \frac{10\theta^4 n}{(\theta^5 + 24)} - \sum x + \sum_{i=1}^n \left(\frac{6\theta^5 + 48}{\theta^6 + 48\theta + 24x^4} \right) \tag{25}$$

set $\frac{d\psi}{d\theta} = 0$ yields the following result

$$\frac{5n}{\theta} - \frac{10\theta^4 n}{(\theta^5 + 24)} - \sum x + \sum_{i=1}^n \left(\frac{6\theta^5 + 48}{\theta^6 + 48\theta + 24x^4} \right) = 0 \tag{26}$$

which has no closed-form solution and hence will be implemented in R using `optim()` function.

distribution and compare it with the following known distributions which are in the class of Lindley distribution.

4 Applications to Real-Life Data

In this section, we will use real-life data sets to illustrate the usefulness of the proposed XRani

Table 2: List of Competing one-parameter distributions in the class of Lindley

Distribution	$f(x)$	$F(x)$
proposed XRani	$\frac{\theta^5}{(\theta^5+24)^2} [\theta^6 + 48\theta + 24x^4] e^{-\theta x}$	$1 - \left\{ 1 + \frac{24\theta^4 x^4 + 96\theta^3 x^3 + 288\theta^2 x^2 + 576\theta x}{(\theta^5+24)^2} \right\} e^{-\theta x}$
Rani [24]	$\frac{\theta^5}{\theta^5+24} (\theta + x^4) e^{-\theta x}$	$1 - \left[1 + \frac{\theta x(\theta^3 x^3 + 4\theta^2 x^2 + 12\theta x + 24)}{\theta^5+24} \right] e^{-\theta x}$
Shanker [22]	$\frac{\theta^5}{\theta^2+1} (\theta + x) e^{-\theta x}$	$1 - \left[1 + \frac{\theta x}{\theta^2+1} \right] e^{-\theta x}$
XShanker [7]	$\frac{\theta^2}{(\theta^2+1)^2} (\theta^3 + 2\theta x + x) e^{-\theta x}$	$1 - \left[1 + \frac{\theta x}{(\theta^2+1)^2} \right] e^{-\theta x}$
XGamma [21]	$\frac{\theta^2}{1+\theta} \left(1 + \frac{\theta}{2} x^2 \right) e^{-\theta x}$	$1 - \left[1 + \frac{\theta x + \frac{\theta^2 x^2}{2}}{1+\theta} \right] e^{-\theta x}$
Rama [23]	$\frac{\theta^4}{\theta^3+6} (1 + x^3) e^{-\theta x}$	$1 - \left[1 + \frac{\theta^3 x^3 + 3\theta^2 x^2 + 6\theta x}{\theta^3+6} \right] e^{-\theta x}$
Lindley [12]	$\frac{\theta^2}{\theta+1} (1 + x) e^{-\theta x}$	$1 - \left[1 + \frac{\theta x}{\theta+1} \right] e^{-\theta x}$
XLindley [5]	$\frac{\theta^2(2+\theta+x)}{(1+\theta)^2} e^{-\theta x}$	$1 - \left[1 + \frac{\theta x}{(1+\theta)^2} \right] e^{-\theta x}$
Ishita [25]	$\frac{\theta^3}{\theta^3+2} (\theta + x^2) e^{-\theta x}$	$1 - \left[1 + \frac{\theta x(\theta x + 2)}{\theta^3+2} \right] e^{-\theta x}$
Akash [26]	$\frac{\theta^3}{\theta^2+2} (1 + x^2) e^{-\theta x}$	$1 - \left[1 + \frac{\theta x(\theta x + 2)}{\theta^2+2} \right] e^{-\theta x}$
Pranav [11]	$\frac{\theta^4}{\theta^4+6} (\theta + x^3) e^{-\theta x}$	$1 - \left[1 + \frac{\theta x(\theta^2 x^2 + 3\theta x + 16)}{\theta^4+6} \right] e^{-\theta x}$
Chris-Jerry [18]	$\frac{\theta^2}{\theta+2} (1 + \theta x^2) e^{-\theta x}$	$1 - \left[1 + \frac{\theta x(\theta x + 2)}{\theta+2} \right] e^{-\theta x}$

The first application is on Vinyl chloride data from clean upgradient ground-water monitoring wells in (g/L) studied by [27] in table 1.

Table 3: Vinyl chloride data from clean upgradient ground-water monitoring wells in (g/L)

5.1	1.2	1.3	0.6	0.5	2.4	0.5	1.1	8.0	0.8	0.4	0.6	0.9	0.4	2.0	0.5	5.3
3.2	2.7	2.9	2.5	2.3	1.0	0.2	0.1	0.1	1.8	0.9	2.0	4.0	6.8	1.2	0.4	0.2

The measures of model performance for the distributions are the negative Log-Likelihood (NLL), Akaike Information Criterion (AIC), Corrected AIC (CAIC), Bayesian Information Criterion (BIC), Hannan–Quinn information criterion (HQIC), Cramer von Mises (W^*), Anderson Darling (A^*), while the Kolmogorov-Smirnov (K-S) statistic and the p-value determine the fitness of the distribution to the data.

Based on results in table 4, the proposed XRani best fits the Vinyl Chloride data having the highest p – value = 0.638. However, it does not perform any better in parameter estimation as its performance measures are not the least among others.

Table 4: Analytical measures of performance and fitness using the Vinyl Chloride Data

Dist	NLL	AIC	CAIC	BIC	HQIC	W^*	A^*	K-S	P-value	θ
XRani	58.06	118.115	118.240	119.641	118.635	0.142	0.877	0.128	0.638	1.602
Xgamma	56.49	114.970	115.095	116.497	115.491	0.079	0.511	0.138	0.533	1.031
Lindley	56.3	114.607	114.732	116.134	115.128	0.063	0.405	0.133	0.588	0.824
Ishita	57.3	116.606	116.731	118.132	117.126	0.095	0.604	0.140	0.514	1.157
Akash	57.57	117.149	117.274	118.676	117.670	0.099	0.630	0.157	0.376	1.166
Chris-Jerry	57.93	117.854	117.979	119.380	118.374	0.103	0.655	0.178	0.230	1.165
Shanker	56.46	114.913	115.038	116.439	115.433	0.064	0.413	0.131	0.607	0.853
Rani	59.88	121.752	121.877	123.278	122.272	0.194	1.165	0.152	0.415	1.784

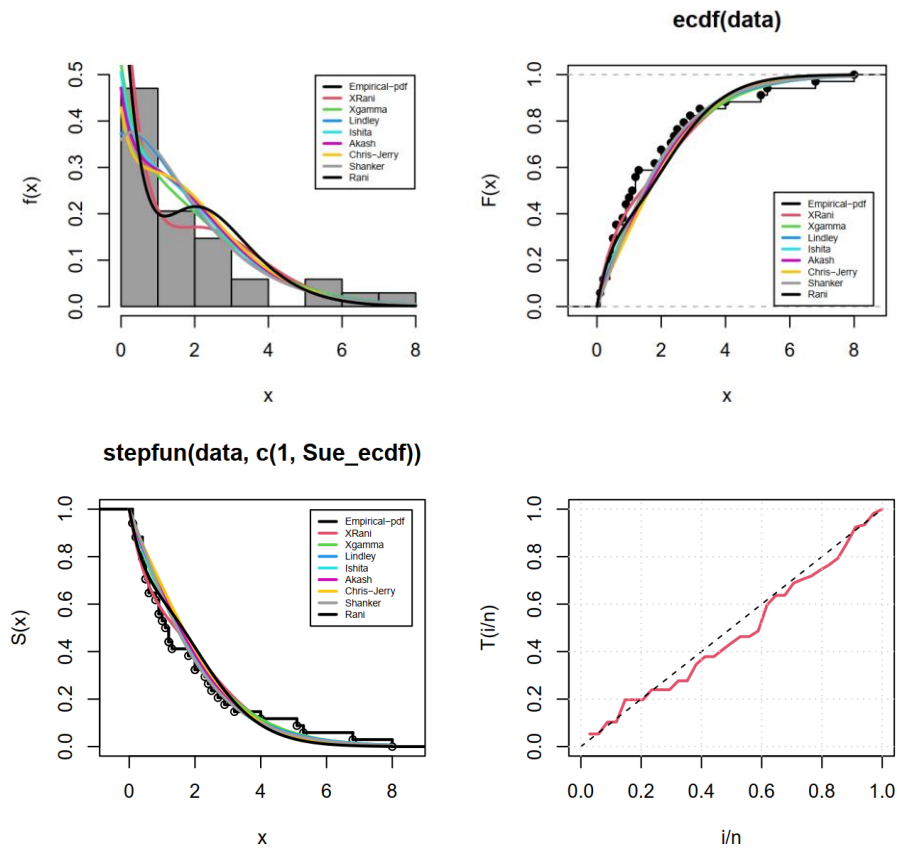


Figure 9: Density, cdf, survival and TTT plots for the Vinyl Chloride data

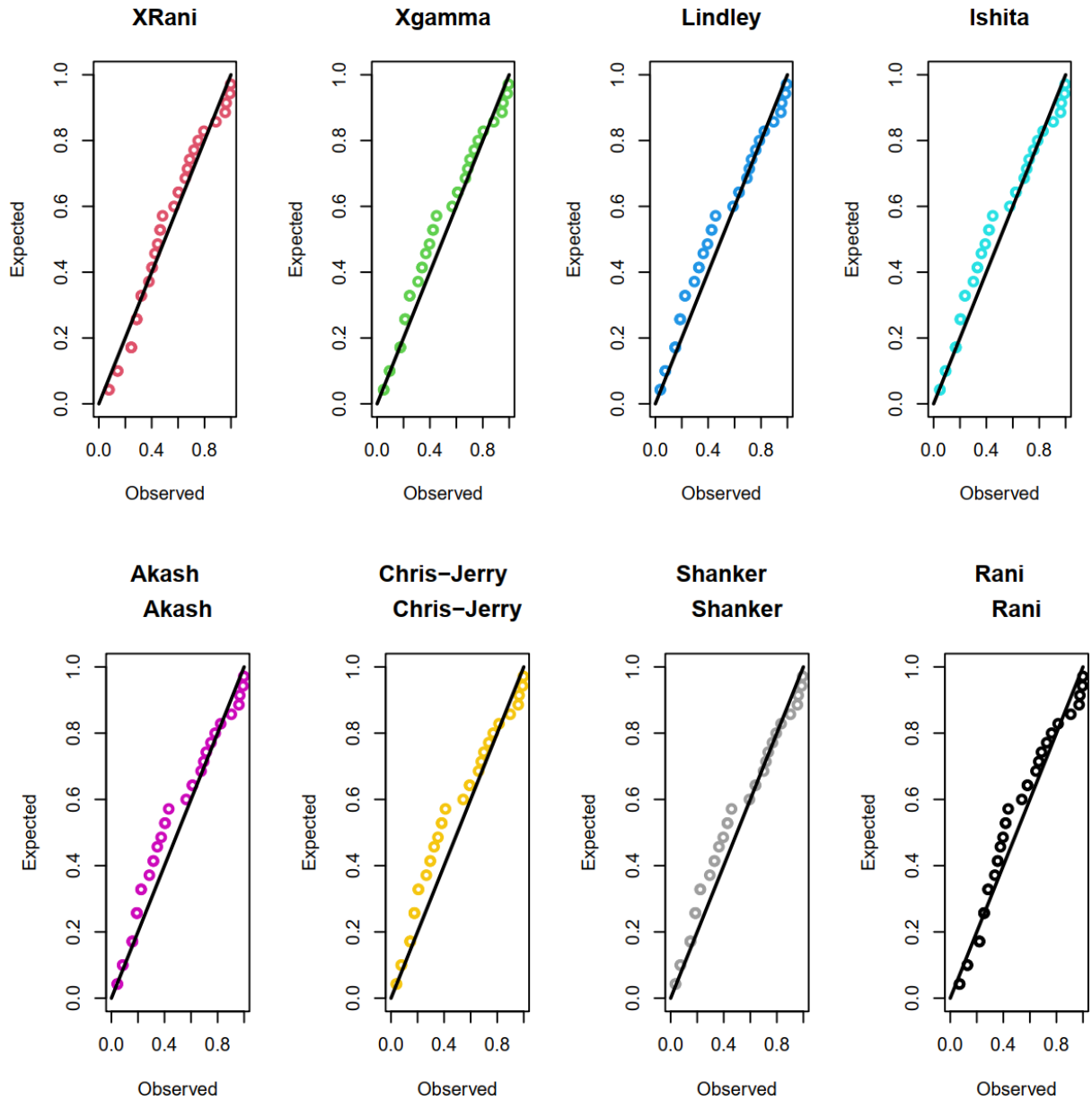


Figure 10: PP plots for the Vinyl Chloride Data

Figures 9 and 10 display the goodness of fit of the selected distributions to the data on the Vinyl chloride data from clean upgradient ground-water monitoring wells in (g/L). The figures show that the XRani distribution fits the data better than other distributions.

The next data represents the Monthly concentration of sulfur dioxide in Long Beach, California studied by [20]. The data are for all the month of March within the period 1956 to 1974, see table 5.

Table 5: Monthly concentration of sulfur dioxide in Long Beach, California in March of 1956 to 1974

21	16	20	15	9	10	10	4	25	18
18	26	25	17	40	55	19	16	9	19.6

In table 6, we fit the XRani distribution including some members of the Lindley class of

distributions to the data on the March concentration of sulfur dioxide in Long Beach.

Table 6: MLEs, Measures of model performance and fitness for the March Sulfur dioxide data

Distr	NLL	AIC	CAIC	BIC	HQIC	W*	A*	θ	K-S	P-value
XRani	73.9	149.802	150.025	150.788	149.997	0.088	0.519	0.255	0.135	0.8608
XGamma	74.44	150.874	151.097	151.870	151.069	0.089	0.547	0.143	0.176	0.5646
Lindley	75.32	152.638	152.860	153.634	152.833	0.088	0.522	0.097	0.209	0.3476
XShanker	74.88	151.755	151.977	152.751	151.949	0.087	0.519	0.101	0.202	0.3911
Chris-Jerry	73.92	149.843	150.065	150.838	150.037	0.088	0.528	0.147	0.165	0.6515
Shanker	74.82	151.630	151.852	152.626	151.825	0.088	0.519	0.101	0.201	0.3917
XLindley	75.81	153.621	153.843	154.617	153.815	0.088	0.527	0.094	0.216	0.3112
Rani	73.90	149.803	150.025	150.799	149.997	0.088	0.519	0.255	0.135	0.8605

Based on results in table 6, the proposed XRani best fits the data on the monthly concentration of sulfur dioxide in Long Beach having the highest $p - value =$

0.8608. It also performs better in parameter estimation as its performance measures are the least among others. Figures 11 and 12 demonstrates the fitness.

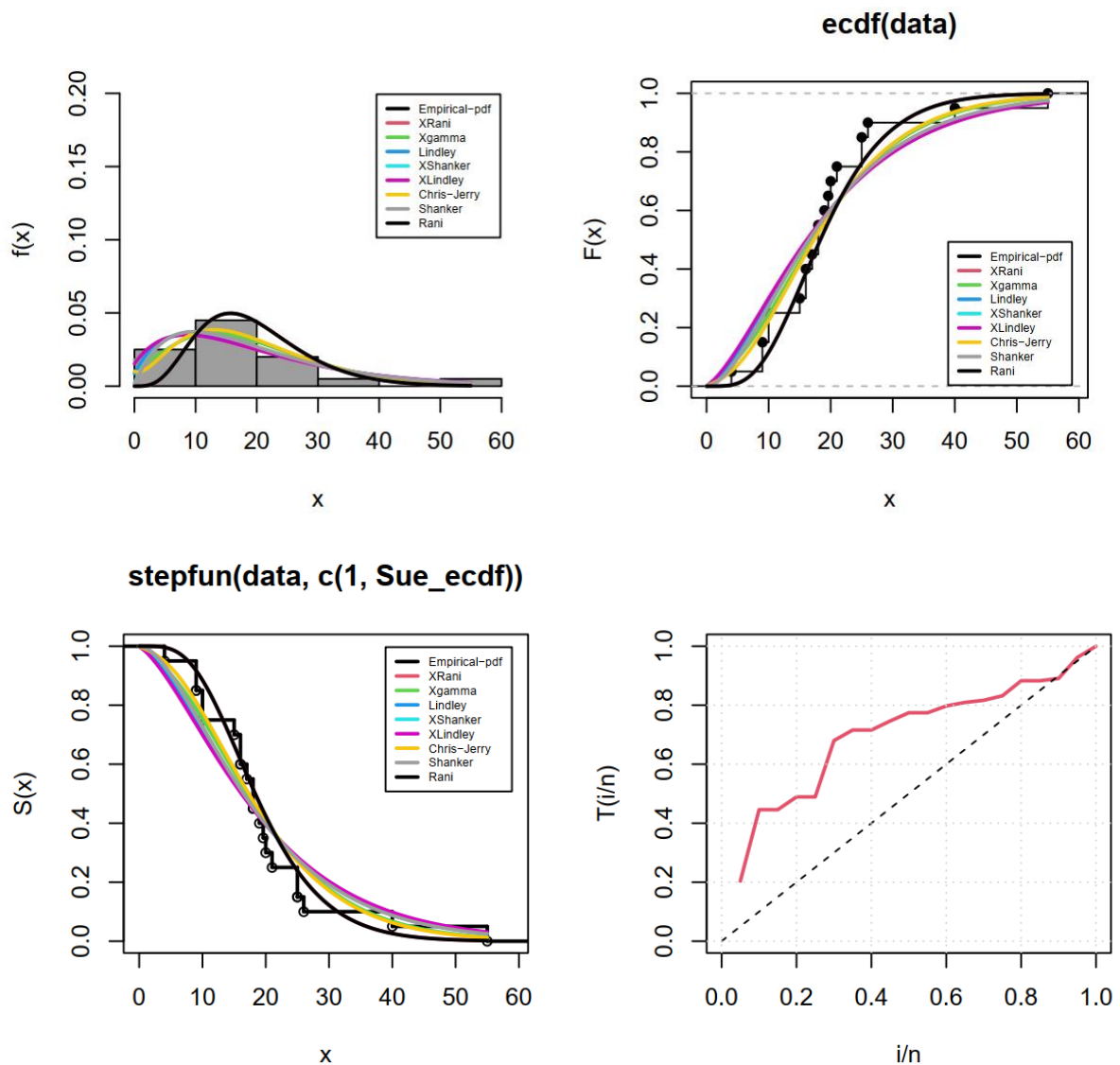


Figure 11: The density, cdf, survival function, and TTT plots of the March Sulfur dioxide data

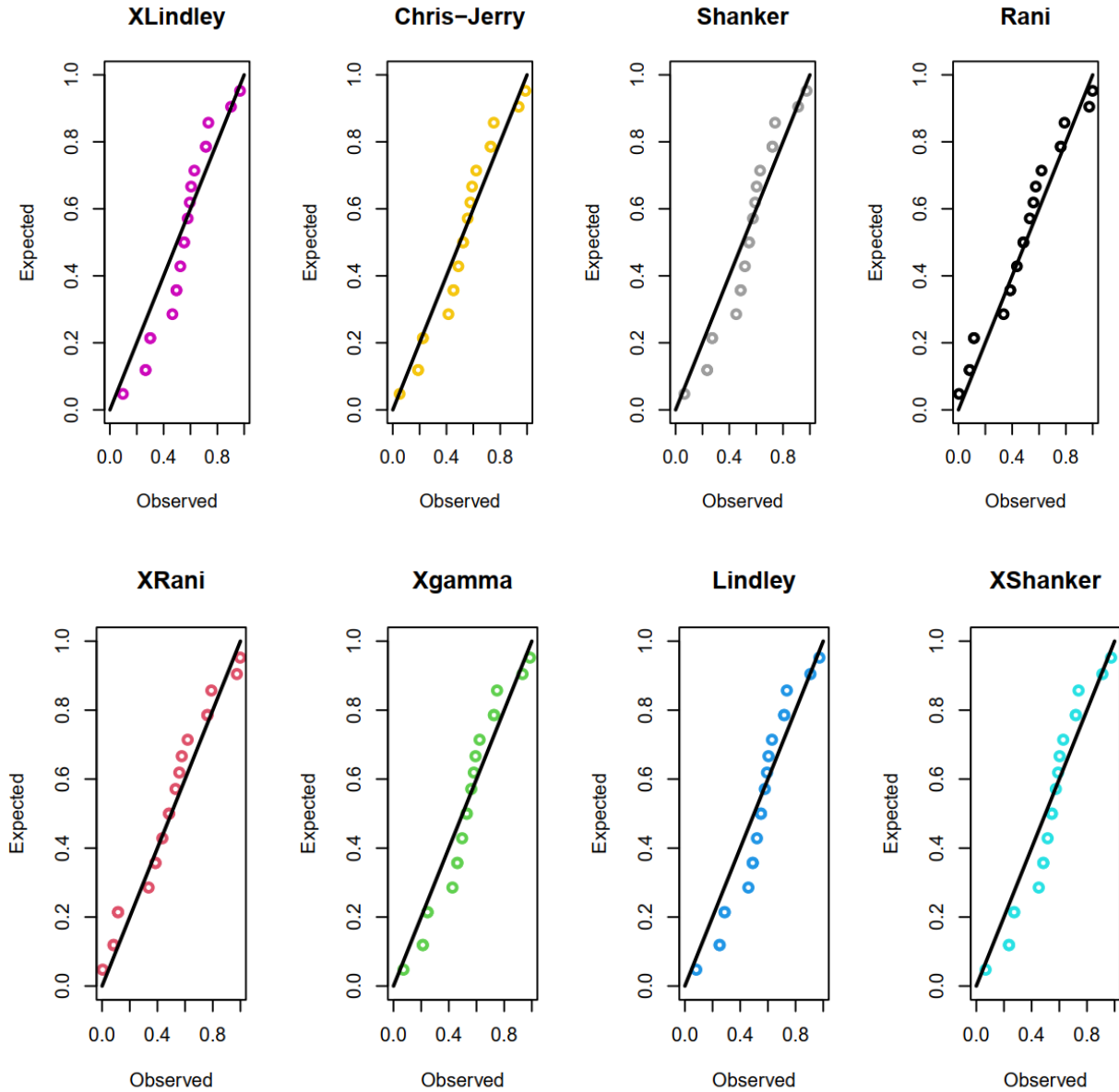


Figure 12: PP plots for the March Sulfur dioxide data

Figures 11 and 12 display the goodness of fit of the selected distributions to the data on the Monthly concentration of sulfur dioxide in Long Beach, California from 1956 to 1974 for the month of March. The figures show that the XRani distribution fits the data better than other distributions.

The next data is on the months of August concentration of sulfur dioxide in Long Beach, California in August spanning 1956 to 1974.

Table 7: Monthly concentration of sulfur dioxide in Long Beach, California in August of 1956 to 1974

44	20	20	20	23	20	15	27	3	9
25	32	18	55	10	20	18	8	9	20.8

In table 8, we fit the XRani distribution including some members of the Lindley class of

distributions to the data on the August concentration of sulfur dioxide in Long Beach.

Table 8: MLEs, measures of model performance and fitness for the Monthly concentration of sulfur dioxide in Long Beach, California in August of 1956 to 1974 for the month of August.

Distr	NLL	AIC	CAIC	BIC	HQIC	W*	A*	θ	K-S	P-value
XRani	77.16	156.320	156.542	157.316	156.514	0.116	0.589	0.240	0.154	0.7288
XGamma	76.12	154.239	154.461	155.234	154.433	0.108	0.566	0.134	0.191	0.4624
Lindley	76.90	155.790	156.012	156.786	155.984	0.114	0.580	0.092	0.219	0.2914
Ishita	75.59	153.181	153.404	154.177	153.376	0.116	0.588	0.144	0.179	0.5404
Akash	75.61	153.212	153.434	154.208	153.407	0.114	0.580	0.143	0.180	0.5393
Chris-Jerry	75.81	153.612	153.834	154.608	153.806	0.110	0.564	0.138	0.184	0.5073
Shanker	76.51	155.017	155.240	156.013	155.212	0.116	0.589	0.095	0.215	0.3129
XLindley	77.29	156.572	156.794	157.567	156.766	0.113	0.577	0.088	0.223	0.2739

Based on results in table 8, the proposed XRani best fits the data on the monthly concentration of sulfur dioxide in Long Beach having the highest $p - value =$

0.07288. However, it does not perform any better in parameter estimation as its performance measures are not the least among others.

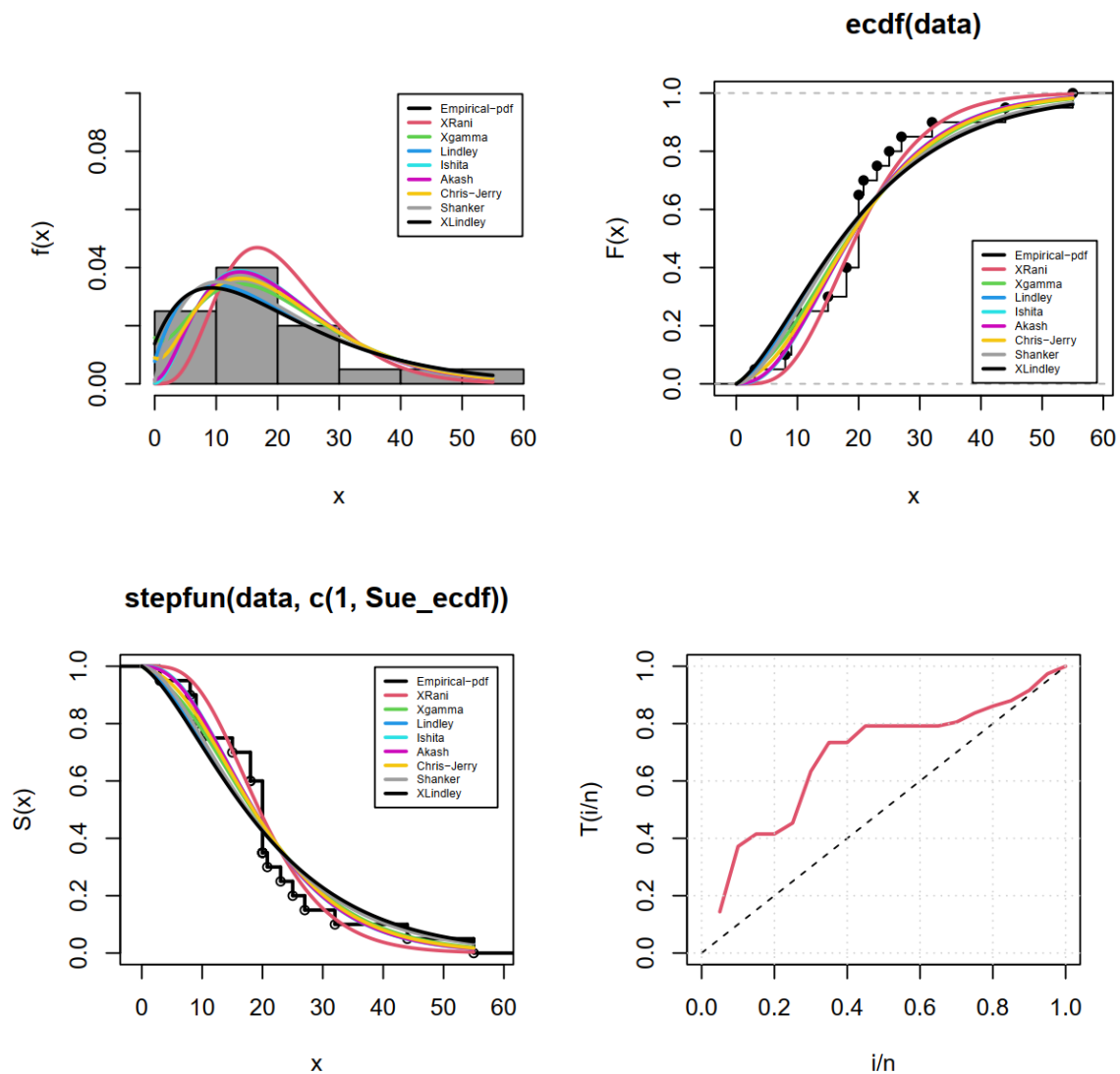


Figure 13: The density, cdf, survival function, and TTT plots of the August Sulfur dioxide data

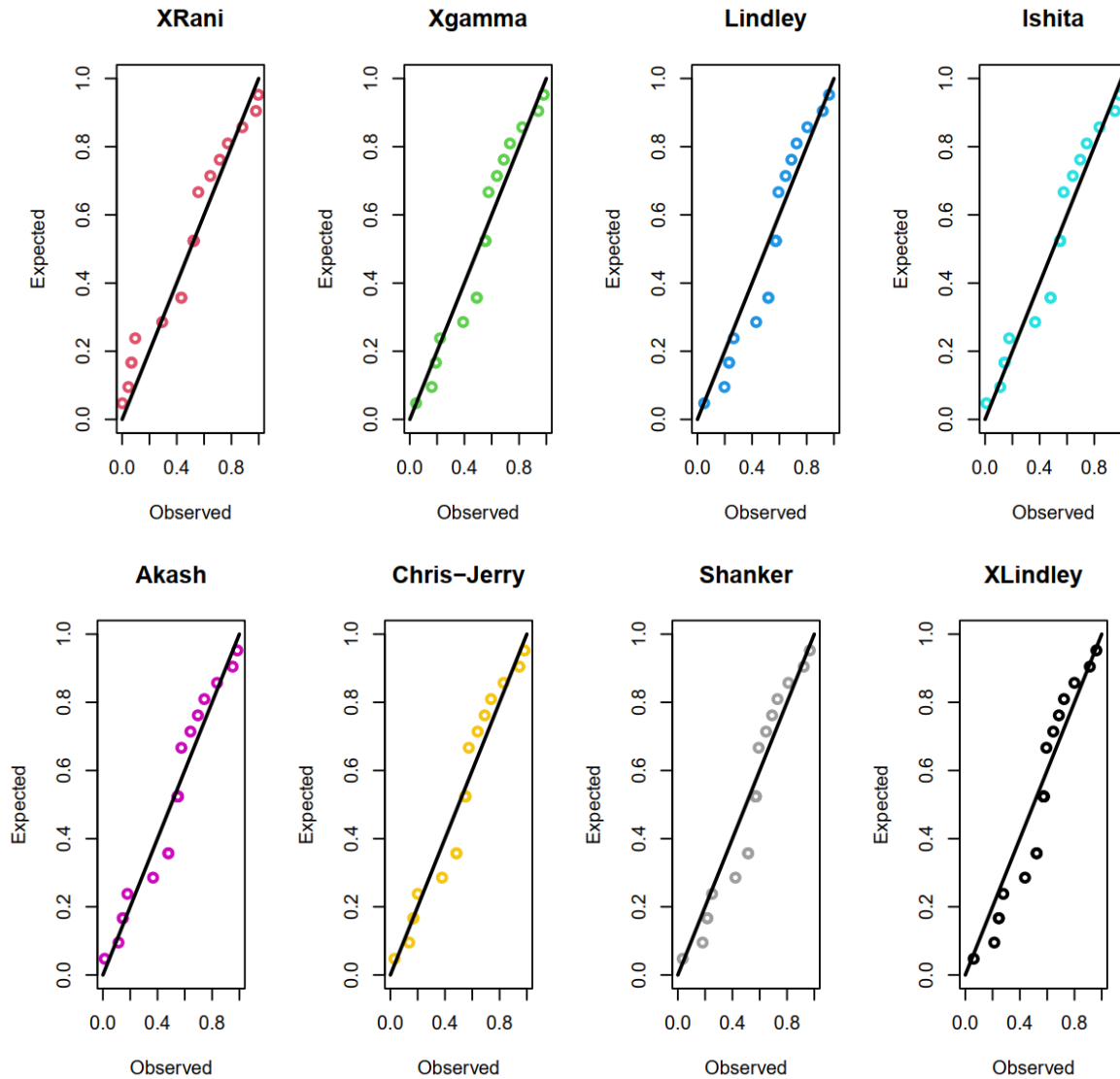


Figure 14: PP plots for the August Sulfur dioxide data

Figures 13 and 14 display the goodness of fit of the selected distributions to the data on the Monthly concentration of sulfur dioxide in Long Beach, California from 1956 to 1974 for the month of August.

The next data is on rainfall reported at the Los Angeles Civic Center from 1943 to 2018 and studied by [13].

Table 9: The rainfall reported at the Los Angeles Civic Center from 1943 to 2018 in the month of March

4.55	2.47	3.43	3.66	0.79	3.07	1.40	0.87	0.44	6.14	0.48	2.99	0.56	1.02
5.30	0.31	0.57	1.10	2.78	1.79	2.49	0.53	2.5	3.34	1.49	2.36	0.53	2.70
3.78	4.83	1.81	1.89	8.02	5.85	4.79	4.10	3.54	8.37	0.28	1.29	5.27	0.95
0.26	0.81	0.17	5.92	7.12	2.74	1.86	6.98	2.16	4.06	1.24	2.82	1.17	0.32
4.32	1.47	2.14	2.87	0.05	0.01	0.35	0.48	3.96	1.75	0.54	1.18	0.87	1.60
0.09	2.69												

In table 10, we fit the XRani distribution including some members of the Lindley class of distributions to the data on rainfall reported at the Los

Angeles Civic Center from 1943 to 2018 in the month of March.

Table 10: MLEs, measures of model performance and fitness for the rainfall data

Distr	NLL	AIC	CAIC	BIC	HQIC	W*	A*	θ	K-S	P-value
XRani	137.47	276.942	276.999	279.219	277.848	0.105	0.627	1.447	0.075	0.8128
Lindley	135.82	273.630	273.687	275.907	274.537	0.026	0.170	0.655	0.080	0.7469
Ishita	136.49	274.979	277.036	277.256	275.886	0.031	0.212	0.978	0.087	0.6457
Akash	136.42	274.838	274.895	277.114	275.744	0.031	0.210	0.965	0.089	0.6172
Pranav	137.63	277.267	277.324	279.543	278.173	0.068	0.433	1.276	0.083	0.7073
Chris-Jerry	136.30	274.596	274.653	276.872	275.502	0.030	0.204	0.946	0.090	0.5999
Rama	138.63	279.261	279.319	281.538	280.168	0.077	0.483	1.303	0.104	0.4206
Rani	140.0	281.990	282.048	284.267	282.897	0.140	0.830	1.584	0.105	0.4056

Based on results in table 10, the proposed XRani best fits the data on the monthly concentration of sulfur dioxide in Long Beach having the highest p –

value = 0.08128. However, it does not perform any better in parameter estimation as its performance measures are not the least among others.

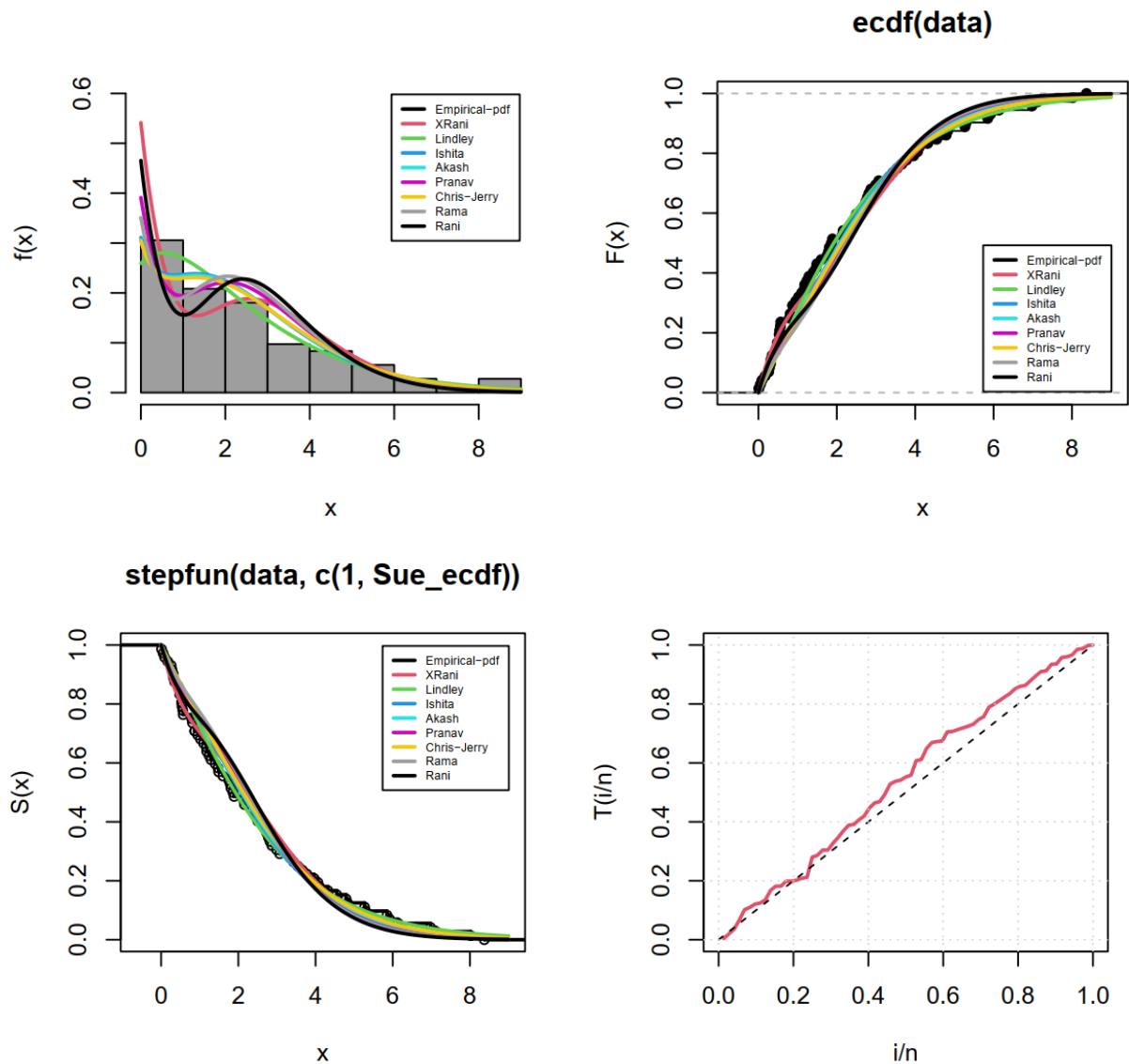


Figure 15: Density, cdf, survival function, and TTT plot for the rainfall data

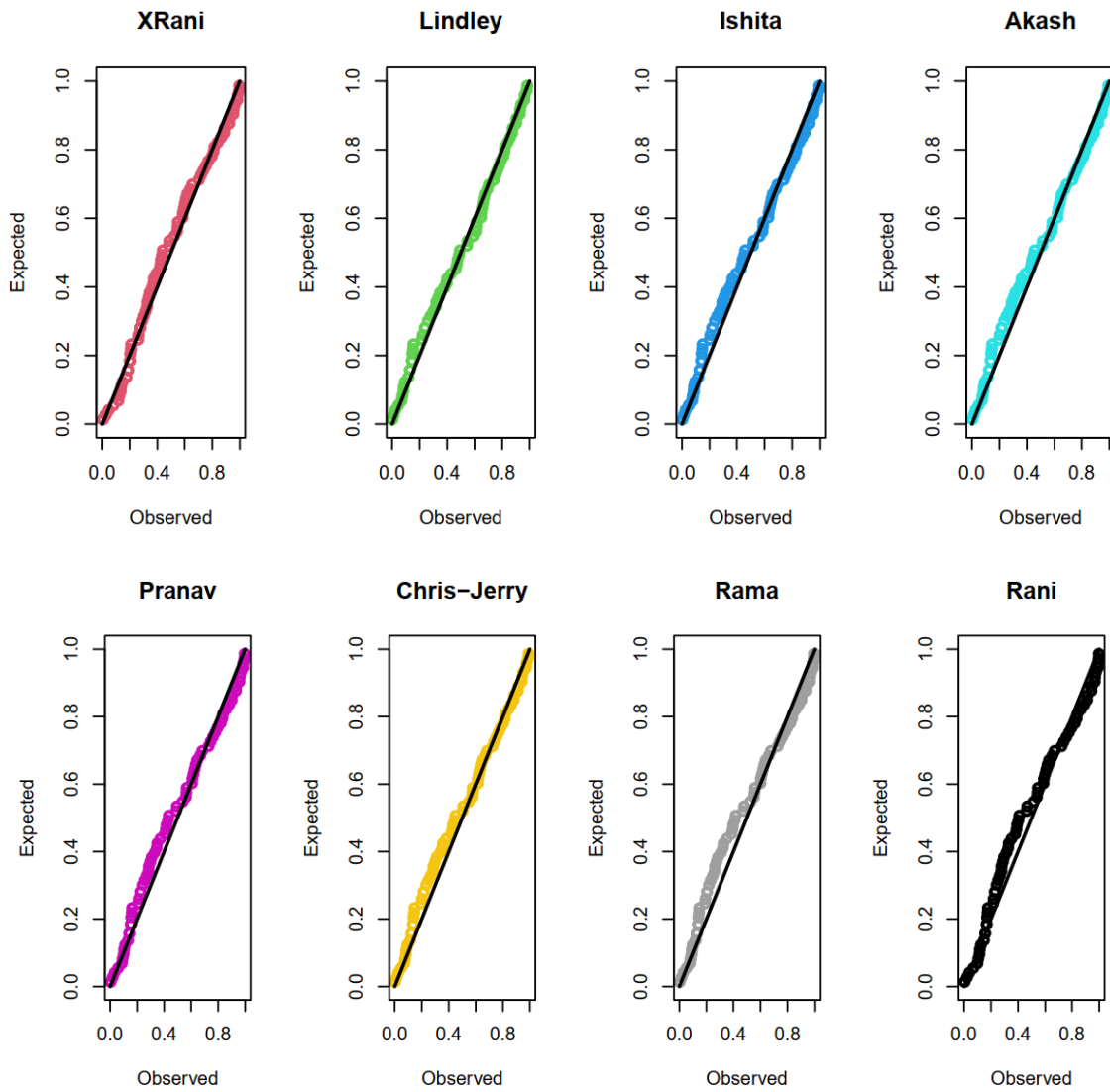


Figure 16: PP plots for the rainfall data

Figures 15 and 16 display the goodness of fit of the selected distributions to the data on rainfall reported

at the Los Angeles Civic Center from 1943 to 2018 in the month of March.

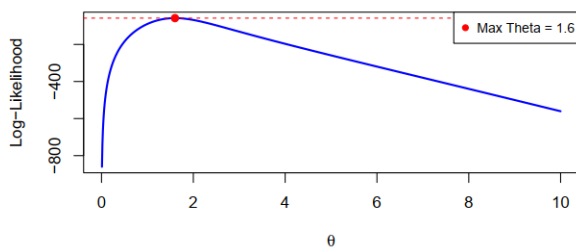


Figure 17: Log-likelihood profile for Vinyl Chloride data

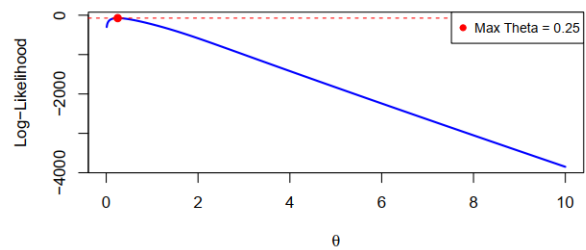


Figure 18: Log-likelihood profile for March sulfur dioxide data

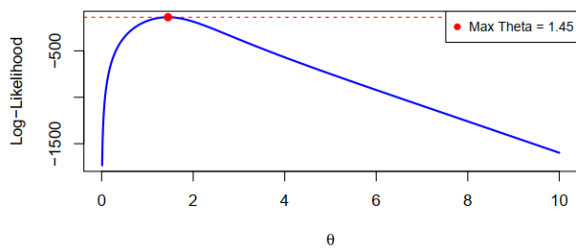


Figure 19: Log-likelihood profile for the rainfall data

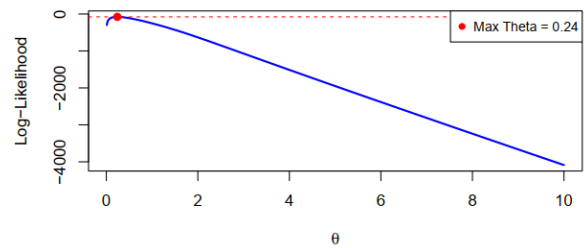


Figure 20: Log-likelihood profile for August sulfur dioxide data

The log-likelihood profile plots in figures 17 to 20 justifies the MLEs estimates in tables 4, 6, 8, and 10.

5. CONCLUSION

In this article, we have proposed a modification of Rani distribution. The new distribution is also a one-parameter distribution which is more flexible in the applications using some data sets in tables 4, 6, 8, and 10. The properties were derived and the proposed distribution parameter was estimated using maximum likelihood estimation. Except in the case of data on the concentration of sulfur dioxide in Long Beach in the months of March from 1956 to 1974, the proposed XRani distribution only best fits the data sets but did not perform better in parameter estimation. Overall, the XRani distribution competes favorably with the members of the Lindley class of distributions.

CONFLICT OF INTEREST

The authors declare that there is no conflict of interest.

ACKNOWLEDGEMENT

The authors appreciate the reviewers and editors whose contributions substantially improved the quality of this article.

FUNDING

The authors declare that this article did not receive any external funding.

REFERENCES

- Said, H. A. (2015). Extended inverse Lindley distribution: properties and application. *Springer Plus* 4, 1–13.
- Anabike, I. C., Igbokwe, C. P., Onyekwere, C. K., & Obulezi, O. J. (2023). Inference on the parameters of Zubair-Exponential distribution with application to survival times of Guinea Pigs. *Journal of Advances in Mathematics and Computer Science*, 38(7), 12-35.
- Bakouch, H. S., Al-Zahrani, B. M., Al-Shomrani, A. A., Marchi, V. A., & Louzada, F. (2012). An extended Lindley distribution. *Journal of the Korean Statistical Society*, 41, 75-85.
- Biju, G. V., Rajagopalan, V., & Kumar, C. S. (2020). On weighted Rani distribution with applications to Bladder cancer data. *High Technology Letters*, 26(6), 546-558.
- Chouia, S., & Zeghdoudi, H. (2021). The xlindley distribution: Properties and application. *Journal of Statistical Theory and Applications*, 20(2), 318-327.
- Elbatal, I., Diab, L. S., & Elgarhy, M. (2016). Exponentiated quasi Lindley distribution. *International journal of reliability and applications*, 17(1), 1-19.
- Etaga, H. O., Celestine, E. C., Onyekwere, C. K., Omeje, I. L., Nwankwo, M. P., Oramulu, D. O., & Obulezi, O. J. (2023). A New Modification of Shanker Distribution with Applications to Increasing Failure Rate Data. *Earthline Journal of Mathematical Sciences*, 13(2), 509-526.
- Ganaie, R. A., & Rajagopalan, V. (2022). Exponentiated Aradhana distribution with properties and applications in engineering sciences. *Journal of Scientific Research*, 66(1), 316-325.
- Ghitany, M. E., Atieh, B., & Nadarajah, S. (2008). Lindley distribution and its application. *Mathematics and computers in simulation*, 78(4), 493-506.
- Innocent, C. F., Frederick, O. A., Udofia, E. M., Obulezi, O. J., & Igbokwe, C. P. (2023). Estimation of the parameters of the power size biased Chris-Jerry distribution. *International Journal of Innovative Science and Research Technology*, 8(5), 423-436.
- Shukla, K. K. (2018). Pranav distribution with properties and its applications. *Biom Biostat Int J*, 7(3), 244–254.
- Dennis, V. L. (1958). Fiducial distributions and Bayes' theorem. *Journal of the Royal Statistical Society. Series B, (Methodological)*, 102–107.
- Nadar, M., & Kızılaslan, F. (2015). Estimation and prediction of the Burr type XII distribution based on record values and inter-record times. *Journal of Statistical Computation and Simulation*, 85(16), 3297-3321.

14. Obulezi, O., Igbokwe, C. P., & Anabike, I. C. (2023). Single acceptance sampling plan based on truncated life tests for zubair-exponential distribution. *Earthline Journal of Mathematical Sciences*, 13(1), 165-181.
15. Obulezi, O. J., Anabike, I. C., Okoye, G. C., Igbokwe, C. P., Etaga, H. O., & Onyekwere, C. K. The Kumaraswamy Chris-Jerry Distribution and its Applications. *Journal of Xidian University*, 17(6), 575–591.
16. Obulezi, O. J., Anabike, I. C., Oyo, O. G., Igbokwe, C., & Etaga, H. (2023). Marshall-Olkin Chris-Jerry distribution and its applications. *International Journal of Innovative Science and Research Technology*, 8(5), 522-533.
17. Al-Omari, A. I., Aidi, K., & Seddik-Ameur, N. (2021). A Two Parameters Rani Distribution: Estimation and Tests for Right Censoring Data with an Application. *Pakistan Journal of Statistics and Operation Research*, 1037-1049.
18. Onyekwere, C. K., & Obulezi, O. J. (2022). Chris-Jerry distribution and its applications. *Asian Journal of Probability and Statistics*, 20(1), 16-30.
19. Oramulu, D. O., Igbokwe, C. P., Anabike, I. C., Etaga, H. O., & Obulezi, O. J. Simulation Study of the Bayesian and Non-Bayesian Estimation of a new Lifetime Distribution Parameters with Increasing Hazard Rate. *Asian Research Journal of Mathematics*, 19(9), 183–211.
20. Pak, A., Raqab, M. Z., Mahmoudi, M. R., Band, S. S., & Mosavi, A. (2022). Estimation of stress-strength reliability $R = P(X > Y)$ based on Weibull record data in the presence of inter-record times. *Alexandria Engineering Journal*, 61(3), 2130-2144.
21. Sen, S., Maiti, S. S., & Chandra, N. (2016). The xgamma distribution: statistical properties and application. *Journal of Modern Applied Statistical Methods*, 15(1), 38.
22. Shanker, R. (2015). Shanker distribution and its applications. *International journal of statistics and Applications*, 5(6), 338–348.
23. Shanker, R. (2017). Rama distribution and its application. *International Journal of Statistics and Applications*, 7(1), 26–35.
24. Shanker, R. (2017). Rani distribution and its application. *Biometrics & Biostatistics International Journal*, 6(1), 1–10.
25. Shanker, R., & Shukla, K. K. (2017). Ishita distribution and its applications. *Biometrics & Biostatistics International Journal*, 5(2), 1–9.
26. Shanker, R. (2015). Akash distribution and its applications. *International Journal of Probability and Statistics*, 4(3), 65–75.
27. Tolba, A. H., Onyekwere, C. K., El-Saeed, A. R., Alsadat, N., Alohal, H., & Obulezi, O. J. (2023). A New Distribution for Modeling Data with Increasing Hazard Rate: A Case of COVID-19 Pandemic and Vinyl Chloride Data. *Sustainability*, 15(17), 12782.
28. Zeghdoudi, H., & Nedjar, S. (2016). Gamma Lindley distribution and its application. *Journal of Applied Probability and Statistics*, 11(1), 129-138.
29. Zitouni, M. (2020). The Kumaraswamy-Rani distribution and its applications. *Journal of Biometrics and Biostatistics*, 11(1), 1–4.